

High Pressure Properties for Electrical Resistivity and Ce Valence State of Heavy-Fermion Antiferromagnet Ce₂NiGa₁₂

N Kawamura¹, R Sasaki², K Matsubayashi², N Ishimatsu³, M Mizumaki¹,
Y Uwatoko², S Ohara⁴, and S Watanabe⁵

¹ Japan Synchrotron Radiation Research Institute, 1-1-1 Kouto, Sayo, Hyogo 679-5198, Japan

² Institute for Solid State Physics, The University of Tokyo, Kashiwa, Chiba 277-8581, Japan

³ Department of Physics, Graduate School of Science, Hiroshima University, 1-3-1
Kagamiyama, Higashi-Hiroshima, Hiroshima 739-8526, Japan

⁴ Department of Engineering Physics, Electronics and Mechanics, Graduate School of
Engineering, Nagoya Institute of Technology, Gokiso, Showa, Nagoya, Aichi 466-8555, Japan

⁵ Quantum Physics Section, Kyushu Institute of Technology, 1-1 Sensui, Tobata, Kitakyushu,
Fukuoka 804-8550, Japan

E-mail: naochan@spring8.or.jp

Abstract. A heavy-fermion antiferromagnet Ce₂NiGa₁₂ has been studied at a viewpoint of pressure effects. Electrical resistivity measurements show that the antiferromagnetic ordering is suppressed at $P_C \sim 5.5$ GPa, and that Fermi liquid behaviour is observed above P_C . To investigate how Ce valence state is associated with the observed critical phenomena, X-ray absorption spectra at Ce L_3 -edge have been performed. Ce valence state drastically varies at $P_v \sim 9$ GPa in the initial applying pressure process, whereas anomalous behaviour is not observed in the Ce valence under pressures around P_C . Consequently, the quantum critical phenomena in Ce₂NiGa₁₂ around P_C is not strongly connected with Ce valence state.

1. Introduction

Quantum criticality phenomena have attracted much attention for exotic physical properties such as spin and orbital ordering, unconventional superconductivity, and magnetic phase transitions. Such phenomena have been observed in many Ce intermetallic compounds [1]. In particular, the unconventional superconductivity often appears near a quantum critical point (QCP), at which the magnetic order disappears. Moreover, the QCP can be controlled by external fields such as pressure and magnetic field since a competition between RKKY interaction and Kondo effect has an influence on the QCP. Recently, several theoretical approaches for the unconventional superconductivity have been proposed [2–4]. Among them, importance of valence transition near the QCP is predicted [3], and a number of experimental efforts for valence transition have been performed in Ce intermetallic compounds [5, 6]. However, an association of the QCP with the valence transition still remains as an open question.

Pressure as external fields provides large energy to the electron system compared with magnetic field because pressure directly affects band structure through the hybridization of electronic states. In fact, pressure-induced heavy-fermion (HF) superconductors have been reported for the Ce-based intermetallic compounds such as CeCu₂Si₂ and CeCoIn₅ whose crystallized symmetry is tetragonal [7, 8]. Ce₂MGa₁₂ (M =Ni, Pd, and Pt) also crystallizes in the tetragonal symmetry (space group $P4/nbm$), and the Ce atom is aligned in a two-dimensional square lattice site perpendicular to the c -axis [9].



Moreover, these compounds have been reported as HF antiferromagnets with Néel temperature $T_N = 10$, 11, and 7 K the ground state at ambient pressure (AP) for $M = \text{Ni}$, Pd , and Pt , respectively. Therefore, it is important to investigate the properties of isostructural Ce compounds for understanding the quantum criticality behavior from a view point of Ce valence state.

To capture the valence transition, X-ray absorption spectroscopy (XAS) at Ce L_3 -absorption edge is suitable for observation of pressure effect because chemical shift occurs in the spectrum due to valence transition [10]. To study the quantum criticality of $\text{Ce}_2\text{NiGa}_{12}$ and its Ce valence state, the electrical resistivity and XAS measurements were performed under high pressure and low temperature.

2. Experimental

Single crystals of $\text{Ce}_2\text{NiGa}_{12}$ is synthesized by a gallium self-flux method [11]. Crystal structure with tetragonal $P4/nbm$ is confirmed by the X-ray powder diffraction using Cu $K\alpha$ line. Estimated lattice parameters, $a = 0.6108$ nm and $c = 1.5506$ nm, are slightly larger than those of previous report [9]. The electrical resistivity measurements at high pressure were performed by Palm Cubic Anvil Cell. Gasket of MgO and pressure medium of glycerin were used. Pressure is applied up to 8.0 GPa in a temperature range of 0.45 ~ 300 K. The residual resistivity ratio was evaluated to be ~14 at AP.

Diamond-Anvil-Cell (DAC) is often used as a high-pressure cell for XAS measurements. A compact DAC with $\phi 23.5 \times 17$ mm made of CuBe alloy was used to achieve lower temperature below 10 K. This compact DAC can be easily inserted to the superconducting magnet or cryostat. Pressure variation between 300 K and 4 K depends on the culet size of anvils. The variation of 30~40% and 5~10% was observed by using anvils with culet diameter of 300 and 600 μm , respectively.

Nano-Polycrystalline Diamond (NPD) anvils with culet diameter of 300 μm and with height of 1.0 mm were used to avoid glitches in XAS spectra [12, 13]. A tapered hole with depth of 0.7 mm is fabricated to one anvil in pressure direction to increase X-ray intensity. X-ray transmissivity is improved 22 times higher by the fabrication for X-ray energy of 5.72 keV. Within present work, a fabricated NPD anvil withstands pressure of 15 GPa at 3.4 K.

XAS measurements at high pressure were performed at BL39XU of SPring-8 facility [14]. All measurements were carried out in transmission mode using ionization chambers. X-ray beam of 2 (vertical) \times 9 (horizontal) μm^2 is focused on the sample position by Kirkpatrick and Baez mirror [15]. The compact DAC was mounted on the pulse-tube type cryostat and temperature cools down to 3.4 K. A small chip of single crystal was put into the sample room of $\phi 100$ μm , and mixed liquid of methanol:ethanol = 4:1 was used as a pressure-transmitting medium. Pressure at both low temperature and room temperature inside the DAC was estimated by ruby-fluorescence method [16].

3. Results and Discussion

Figure 1 shows a magnetic component of electrical resistivity (ρ_{mag}) dependent on temperature in $\text{Ce}_2\text{NiGa}_{12}$ at selected pressures, where ρ_{mag} is obtained by subtracting the resistivity of the isostructural non-magnetic $\text{La}_2\text{NiGa}_{12}$ compound [9]. ρ_{mag} at AP shows a typical HF feature of Ce compounds, i.e. a cusp peak due to an antiferromagnetic (AFM) ordering at $T_N = 10$ K and a broad maximum due to Kondo scattering at $T_{\text{max}}^{\text{H}} = 60$ K are observed in ρ_{mag} curve. As increasing pressure, the overall ρ_{mag} increases in magnitude whereas the peak position at $T_{\text{max}}^{\text{H}}$ decreases. The T_N decreases with increasing pressure, and another anomaly appears at $T_{N2} < T_N$ above 2.7 GPa. With further increasing pressure, both T_N and T_{N2} are suppressed and no longer visible above 5.8 GPa, indicating the disappearance of AFM ordering at $P_C \sim 5.5$ GPa. At low temperatures near P_C , there appears an additional broad peak at $T_{\text{max}}^{\text{L}}$, which increases with pressure above 5.3 GPa.

The behavior of ρ_{mag} at low temperature region is analyzed according to Fermi-liquid (FL) character, $\rho_{\text{mag}} = \rho_0 + AT^2$, where ρ_0 represents a residual resistance for $\text{Ce}_2\text{NiGa}_{12}$. The pressure dependence of ρ_0 and A values are shown in figure 2(a). Both ρ_0 and A are enhanced with approaching P_C . In addition, $A \propto (T_{\text{max}}^{\text{L}})^{-2}$ relation is also satisfied above 5.8 GPa as shown in figure 2(b). The relationship indicates that FL state realizes in $\text{Ce}_2\text{NiGa}_{12}$ above P_C . Therefore, $T_{\text{max}}^{\text{L}}$ is associate with the Kondo

temperature T_K , which increases with applying pressure as observed in Ce-based HF compounds [17]. Figure 3 shows the pressure-temperature (P - T) phase diagram of $\text{Ce}_2\text{NiGa}_{12}$ drawn by the characteristic temperatures. The P - T phase diagram clearly shows that the FL phase appears around P_C after disappearance of AFM ordering with applying pressure. In addition, the ρ_0 value is enhanced inside the AFM phase (see figure 2(a)). Similar results have been observed in CeAl_2 and CeCu_5Au [18, 19]. It is suggested that the ρ_0 enhancement is attributed to the energy scale of T_K comparable to T_N [4]. Another possibility is that quantum criticality of valence fluctuation induces instability of ρ_0 [3]. In particular, the latter possibility can be explored since the estimation of Ce valence state under high pressure is feasible by XAS measurements.

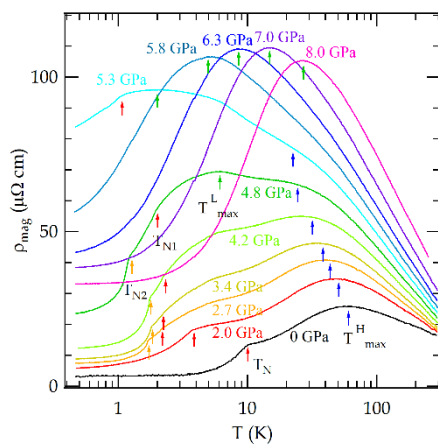


Figure 1. A magnetic component of electrical resistivity ρ_{mag} as a function of temperature in $\text{Ce}_2\text{NiGa}_{12}$ at various pressures.

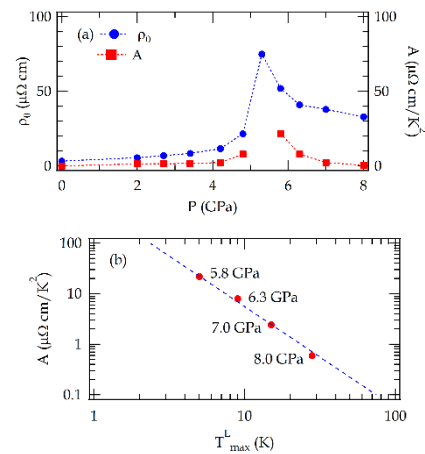


Figure 2. (a) ρ_0 and A coefficient dependent on pressure (see text). (b) A coefficient as a function of T_{max}^L . A broken line denotes $A \propto (T_{\text{max}}^L)^{-2}$.

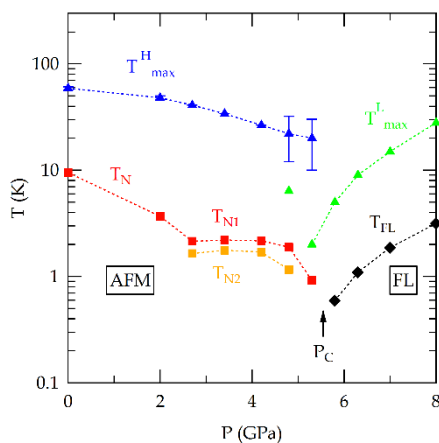


Figure 3. P - T phase diagram in $\text{Ce}_2\text{NiGa}_{12}$ deduced by the electrical resistivity.

Figure 4(a) shows several XAS spectra at the Ce L_3 -edge dependent on pressure at room temperature. The spectral profile at AP indicates Ce trivalent state, reflecting localized f electron feature. As increasing pressure up to 9 GPa, the profile moderately changes with pressure, i.e. a main-peak (called white-line) intensity at 5726.0 eV decreases and the intensity of a shoulder structure at 5735.7 eV increases. This variation is well known as valence variation [10]. However, no anomaly of Ce valence

variation is observed around P_C . Therefore, the quantum critical phenomena in $\text{Ce}_2\text{NiGa}_{12}$ observed by electrical resistivity may not be strongly connected with Ce valence state. On the other hand, a drastic change in XAS profile, in which the shoulder structure at 5735.7 eV becomes clear, is observed above 10 GPa. The phenomenon obviously indicates Ce valence transition.

To elucidate pressure-dependent Ce valence, XAS profiles were analyzed by the profile fitting method as shown in figure 4(b). The averaged Ce valence is obtained by the rate of Ce^{4+} content to Ce^{3+} one. The result estimated by the fitting is shown in figure 4(c). Ce valence is almost trivalent at AP. The valence moderately increases with pressure up to $P_v \sim 9$ GPa, and is suddenly enhanced above P_v . The change rate is comparable to the case in Ce γ - α transition [20]. Here, it is necessary to distinguish the spectral change due to valence variation from the effect of lattice compression according to the Natoli's rule, $k \cdot r = \text{constant}$, where k and r represent X-ray wave number ($\propto E^{-1/2}$) and interatomic distance, respectively [21]. Natoli's rule gives energy shifts for XAS profile so that moderate variation of Ce valence below P_v seems to be the effect of Natoli's rule.

Ce valence state was investigated for pressure-decreasing process. As shown in figure 4(c), Ce valence returns to the previous state for pressure-decreasing process. However, Ce valence for reapplying process is different from that for initial applying-pressure process. On the other hand, the result in another sample is the same as the pressure variation for both increasing and decreasing processes. The difference is attributed to the strain of sample for powderization of single crystal. The situation is often observed in intermetallic compounds such as $\text{CeCu}_{6-x}\text{Au}_x$ [22]. In fact, different pressure dependence is observed in Ce valence state when pressure decreases after applying above P_v . The crystal structure of $\text{Ce}_2\text{NiGa}_{12}$ might change above P_v . Note that the sample for electrical resistivity measurements is corresponding to the initial applying process because of no strain for shape forming. Further investigation such as X-ray powder diffraction and/or electrical resistivity measurements are necessary to discuss Ce valence state in higher pressure region above P_v .

XAS measurements at low temperature were also performed. We succeeded in measuring at 3.4 K up to 15 GPa. Unfortunately, the measurements were performed for only reapplying process. Within current results, no temperature dependence of Ce valence was observed. In addition, pressure dependence at low temperature is as same as the result at room temperature.

For $\text{Ce}_2\text{NiGa}_{12}$, absence of obvious valence transition near P_C provides no correlation between the quantum critical phenomena and Ce valence state. The situation might be similar to the case of CeCu_2Si_2 , in which the different characteristic pressures P_C and P_v are located on two superconducting domes in P - T phase diagram [23]. Moreover, it seems that P_v agrees the pressure which $T_{\text{max}}^{\text{H}}$ merges into $T_{\text{max}}^{\text{L}}$. To ensure the appearance of P_v , low temperature measurements are required for the initial applying-pressure process. Additionally, structural information and electrical resistivity at higher pressure are desired since the drastic variation of Ce valence above P_v is curious.

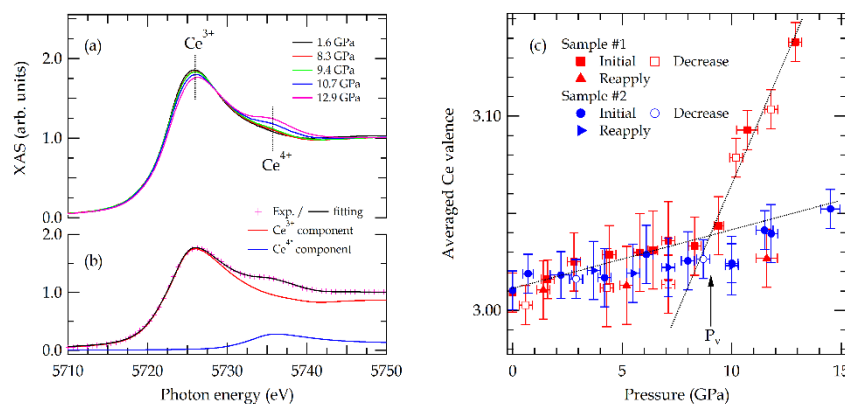


Figure 4. (a) Ce L_3 -XAS spectra in $\text{Ce}_2\text{NiGa}_{12}$ at 300 K at selected pressures. (b) Fitting result of the XAS spectrum at 12.9 GPa for Ce valence estimation. (c) Averaged Ce valence dependent (300 K) on pressure estimated by analysing Ce L_3 -XAS spectra.

4. Conclusion

The electrical resistivity and XAS measurements at Ce L_3 -edge in $\text{Ce}_2\text{NiGa}_{12}$ were performed under high pressure. Quantum criticality phenomena were observed at $P_C \sim 5.5$ GPa in the electrical resistivity. To investigate a relationship between Ce valence state and the quantum criticality, XAS spectra up to 15 GPa were analyzed. Ce valence is drastically enhanced above $P_V \sim 9$ GPa only in the initial applying pressure process. The result indicates that Ce valence variation is not directly associated with the quantum criticality in $\text{Ce}_2\text{NiGa}_{12}$ around P_C . Detailed study of electrical resistivity and crystal structure determination above P_V is necessary to discuss about the Ce valence variation.

Acknowledgements

We thanks to Drs. H. Sumiya and T. Irifune for providing the NPD anvils. This study was performed with the approval of the Japan Synchrotron Radiation Research Institute (JASRI) (Proposal Nos. 2012A1843, 2012B1976, 2013B0046, 2013B1922 and 2014A0046). This work is partially supported by a Grants-in-Aid for Scientific Research (C) (No. 24540389) from the Ministry of Education, Culture, Sports, Science, and Technology (MEXT), Japan.

References

- [1] Doniach S 1977 *Valence Instability and Related Narrow Band Phenomena* ed R D Parks (New York: Plenum)
- [2] Misawa T, Yamaji Y and Imada M 2009 *J. Phys. Soc. Jpn.* **78** 084707
- [3] Watanabe S and Miyake K 2010 *Phys. Rev. Lett.* **105** 186403
- [4] Hattori K and Miyake K 2010 *J. Phys. Soc. Jpn.* **79** 073702
- [5] Rueff J –P, Raymond S, Taguchi M, Sikora M, Itié J –P, Baudelet F, Braithwaite D, Knebel G and Jaccard D 2010 *Phys. Rev. Lett.* **106** 186405
- [6] Yamaoka H, Tsujii N, Yamamoto K, Oohashi H, Vlaicu A M, Kunitani K, Uotani K, Horiguchi D, Tochio T, Ito Y and Shin S 2007 *Phys. Rev. B* **76** 075130
- [7] Assmus W, Herrmann M, Rauchschwalbe U, Riegel S, Lieke W, Spille H, Horn S, Weber G, Steglich F and Cordier G 1984 *Phys. Rev. Lett.* **52** 469
- [8] Petrovic C, Pagliuso P G, Hundley M F, Movshovich R, Sarrao J L, Thompson J D, Fisk Z and Monthoux P 2001 *J. Phys.: Condens. Matter* **13** L337
- [9] Cho J Y, Millican J N, Capan C, Sokolov D A, Moldovan M, Karki A B, Young D P, Aronson M C and Chan J Y 2008 *Chem. Mater.* **20** 6116
- [10] Wohllleben D and Röhler J 1984 *J. Appl. Phys.* **55** 1904
- [11] Ohara S, Yamashita T, Shiraishi T, Matsubayashi K and Uwatoko Y 2012 *J. Phys.: Conf. Ser.* **400** 042048
- [12] Irifune T, Kurio A, Sakamoto S, Inoue T and Sumiya H 2003 *Nature* **421** 806
- [13] Ishimatsu N, Matsumoto K, Maruyama H, Kawamura N, Mizumaki M, Sumiya H and Irifune T 2012 *J. Synchrotron Rad.* **19** 768
- [14] Kawamura N, Ishimatsu N and Maruyama H, 2009 *J. Synchrotron Rad.* **16** 730
- [15] Yumoto H, Hirata K, Nisawa A, Ueno G, Sato M, Son J –Y, Koganezawa T, Machida M, Muro T, Hirosawa I, Suzuki M, Kawamura N, Mizumaki M, Ohashi H, Yamamoto M, Watanabe Y and Goto S 2009 *Proc. SPIE* **7448** 74480Z
- [16] Mao H K, Bell P M, Shaner J W and Steinberg D J 1978 *J. Appl. Phys.* **49** 3276
- [17] Pfleiderer C 2009 *Rev. Mod. Phys.* **81** 1551
- [18] Barbara B, Beille J, Cheaito B, Laurant J M, Rossignol M F, Waintal A and Zemirli S 1987 *J. Phys. France* **48** 635
- [19] Wilhelm H, Raymond S, Jaccard D, Stockert O, Löhneysen H v and Rosch A 2001 *J. Phys. Condens. Matter.* **13** L329
- [20] Rueff J –P, Itié J –P, Taguch M, Hague C F, Mariot J –M, Delaunay R, Kappler J –P and Jaoen N 2006 *Phys. Rev. Lett.* **96** 237403
- [21] Natoli C R 1983 *EXAFS and Near Edge Structure, Springer Series in Chemical Physics* ed A Bianconi, L Incoccia and S Stipcich (Berlin: Springer)
- [22] Hirose Y, *Private communications*
- [23] Holmes A T, Jaccard D and Miyake K 2007 *J. Phys. Soc. Jpn.* **76** 051002